AGRICULTURE AND NATURAL RESOURCES

Journal homepage: http://anres.kasetsart.org

Research article

Assessing climate change impacts on meteorological drought indices for agricultural areas in Chi River Basin, Thailand: Comparative analysis of standardized precipitation index and standardized precipitation evapotranspiration index

Thanasit Promping, Chutipat Foyhirun, Tawatchai Tingsanchali*

Sustainable Water Resources Development Research Group (SWRD), Department of Civil Engineering, Faculty of Engineering at Sriracha, Kasetsart University Sriracha Campus, Chonburi 20230, Thailand

Article Info

Article history:
Received 10 January 2025
Revised 5 May 2025
Accepted 1 July 2025
Available online 31 July 2025

Keywords:
Chi River Basin,
Climate change projection,
Drought,
Standardized precipitation evapotranspiration index (SPEI),
Standardized precipitation index (SPI)

Abstract

Importance of the work: Meteorological drought indices play a critical role in understanding the impact of climate change on water resources.

Objectives: To assess meteorological drought indices under future climate change impact in the Chi River Basin, a drought-prone region in northeast Thailand.

Materials and Methods: The responses to projected climate changes were elucidated for the widely used standardized precipitation index (SPI) and standardized precipitation evapotranspiration index (SPEI). Projections indicated shifts in rainfall and temperature based on three regional climate models (ACCESS, CNRM and MPI) under two commonly used climate change representative concentration pathways (RCP4.5 and RCP8.5).

Results: Analysis of the SPI and SPEI values derived from computed monthly data for 1 mth, 3 mth and 6 mth drought intervals indicated a temporal shift in drought conditions. Specifically, SPI exhibited a dry-to-wet-to-dry pattern across the 2020s, 2050s, and 2080s, while SPEI showed a persistent wet condition in the 2020s and 2050s, followed by a shift to dry conditions in the 2080s. Strong positive correlations (Pearson's correlation coefficient = 0.86–0.97) between SPI and SPEI were observed from the 1990s to the 2080s. The SPI signaled potential drought events across all agricultural areas, while the SPEI indicated unaffected or wet conditions. However, the SPEI had a slower response to changes in drought conditions compared to the SPI. Model performance for both the SPI and SPEI showed unsatisfactory alignment with observed data under RCP4.5 and RCP8.5 during 2011−2020.

Main finding: SPI and SPEI values can be used as components of a composite drought indicator, aligning with recommendations from the World Meteorological Organization and the Global Water Partnership in 2016 for a multi-indicator approach to provide a comprehensive representation of all drought types.

* Corresponding author.
E-mail address: tawatchai@eng.src.ku.ac.th (T. Tingsanchali)

https://doi.org/10.34044/j.anres.2025.59.4.11

Introduction

In recent times, there have been marked changes in global climate parameters, such as rainfall, temperature and evaporation, as evidenced in Intergovernmental Panel on Climate Change, 2021). For example, the mean global surface temperature was approximately 1.09°C higher in 2011−2020 compared to 1850−1900, with a more pronounced increase over land areas (1.59°C) than over the ocean (0.88°C). Furthermore, global average rainfall over land areas has slightly increased since 1950, with a more rapid increase observed since the 1980s. Climate change has substantially impacted water resources within the hydrological cycle and natural disaster management (Schulze, 2000; Zhao et al., 2009; Shrestha et al., 2016). The rise in greenhouse gas emissions from human activities is a primary cause of current climate change (Zhao et al., 2009; Yang et al., 2016; Shrestha et al., 2021). Thailand has been severely affected by water-related disasters, such as floods and droughts annually and these are expected to become more unpredictable and challenging to manage in the future. For example, in 2021, a drought disaster in Thailand considerably reduced the total water capacity in main rivers and reservoirs, leading to a loss of soil moisture anomalies across land surface areas which had a profound impact on the 11 million people engaged in farming and crop production (Promping and Tingsanchali, 2025). Historically, the Chi River Basin (CRB) has experienced substantial droughts, impacting an estimated 1.54 million people and 0.42 million households in 2014, with the impact of droughts being particularly severe in 2008 and 2012, with more than 2.5 million people affected each year (Department of Disaster Prevention and Mitigation, 2025).

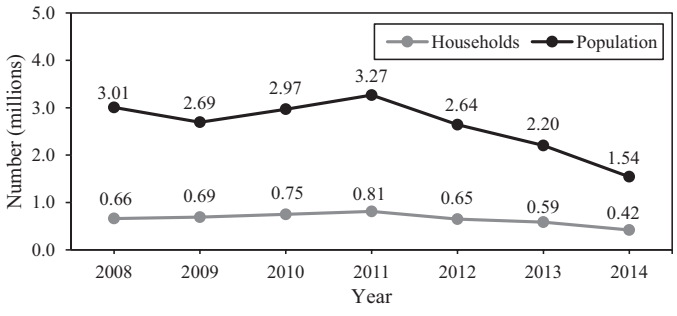

Fig. 1 Number of drought-affected households and population 2008–2014; sourced: Department of Disaster Prevention and Mitigation (2025)

Pei et al. (2020) reported on drought indices that involved a comparative analysis of both the standardized precipitation index (SPI) and the standardized precipitation evapotranspiration index (SPEI), in Inner Mongolia, China. Their study analyzed the drought hazard impact using data from 102 meteorological stations over 1 mth, 3 mth, 6 mth and 12 mth time scales during 1981−2018. They found that both the SPI and SPEI tended to increase slightly, with the SPEI being more suitable for drought monitoring in Inner Mongolia. Homdee et al. (2016) conducted a comparative performance analysis of three climate drought indices (SPI, SPEI and the standardized precipitation actual evapotranspiration index, SPAEI) during 1951−2009 in the Chi River Basin, Thailand. Their study concluded that the SPEI and SPAEI had similar values and performed better than the SPI regarding agricultural production. Given these findings, the current study aimed to predict and compare future drought indices (SPI and SPEI) under climate change projections with different representative concentration pathways. The climate projection method simulated daily rainfall and maximum and minimum temperatures for 1970–2010 (historical) and 2011–2100 (future) periods, using three regional climate models (ACCESS, CNRM, MPI) under two representative concentration pathways (RCP4.5 and RCP8.5). However, the SPI and SPEI are generally used as drought indices for monitoring present drought and shortage impacts on agricultural areas with different drought time scales: 1 mth for rice, 3 mth for field crops (cassava, maize, sugarcane) and 6 mth for orchards or perennial crops (coconut, longan, mango, rubber plantation). The sub-objectives of the current study were: 1) to evaluate future climate projections using a linear bias correction formula; 2) to estimate the SPI from future monthly rainfall; 3) to investigate the SPEI using monthly rainfall and maximum and minimum temperatures; and 4) to compare both drought hazard indices with historical and future time steps: past (the 1990s, 1981–2010); near-term (the 2020s, 2011−2040); mid-term (the 2050s, 2041−2070); and long-term (the 2080s, 2071−2100).

Materials and Methods

Study area and data collection

The Chi River Basin (CRB) is located in northeast Thailand and has a population of 6.6 million people. It covers 14 provinces and drains from west to east, with a river length of 830 km, meeting the Mun River in Ubon Ratchathani province

before flowing into the Mekong River. The drainage area is approximately 49,000 km², consisting of 60% agricultural area, 31% forest area, 2.9% urban area, 2.5% water body area and 3.5% other (Prakongsri and Santiboon, 2020). Rice and field crops dominate the agricultural sector, covering more than 41% of the paddy field area. The topography features a large flat-sloped area in the middle and lower parts, with a range of 103–1,292 m above mean sea level (Fig. 2). The Chi River originates from the Dong Phaya Yen Range, located between the Pasak-Chi River Basin borders in the upper part of the CRB. The middle and lower parts of the CRB have extensive agricultural areas, mainly paddy fields, field crops (cassava, maize, sugarcane), orchards (coconut, longan, mango,) and rubber tree plantations. The region has a tropical climate (Homdee et al., 2016) with annual average rainfall of approximately 1,280 mm and average maximum and minimum temperatures of 35.9°C and 16.9°C, respectively (Hydro-Informatics Institute, 2025). The climate can be divided into three seasons: winter (November–February), summer (March–mid May) and rainy (mid May–October).

Climatic data for this study was gathered from six meteorological stations, measured by the Thai Meteorological Department (TMD) and the Royal Irrigation Department of Thailand (RID) from Kuntiyawichai et al. (2020). These data consisted of observed daily rainfall and maximum and minimum temperatures during 1970–2010. Three different regional climate models (RCMs) were applied to simulate future climate change projections: ACCESS-CSIRO-CCAM, CNRM-CM5-CSIRO-CCAM and MPI-ESM-LR-CSIRO-CCAM (Promping and Tingsanchali, 2020; Shrestha et al., 2020; Boonwichai et al., 2021) (developed by the Collaboration for Australian Weather and Climate Research, the National Centre for Meteorological Research and the European Network of Earth System Modelling, respectively) with high resolution (0.50° × 0.50°/d) under two commonly used climate change representative concentration pathways (RCP4.5 and RCP8.5) from 1970–2100. The data were obtained from the CORDEX (South Asia) data portal (http://cccr.tropmet.res.in/home/index.jsp) (Ghimire et al., 2021). Data on the affected areas of past drought events (2011−2020) were collected as points (approximately 434 and 263 locations for drought and non-drought locations, respectively), based on Department of Disaster Prevention and Mitigation (2025).

Methodology

The overall methodology was divided into four steps: 1) climate projection method from daily rainfall and maximum and minimum temperatures; 2) investigating the SPI using monthly rainfall; 3) evaluating the SPEI from monthly rainfall and maximum and minimum temperatures; and 4) comparing future drought indices (SPI and SPEI) under the different RCP4.5 and RCP8.5 scenarios (Boonwichai et al., 2018).

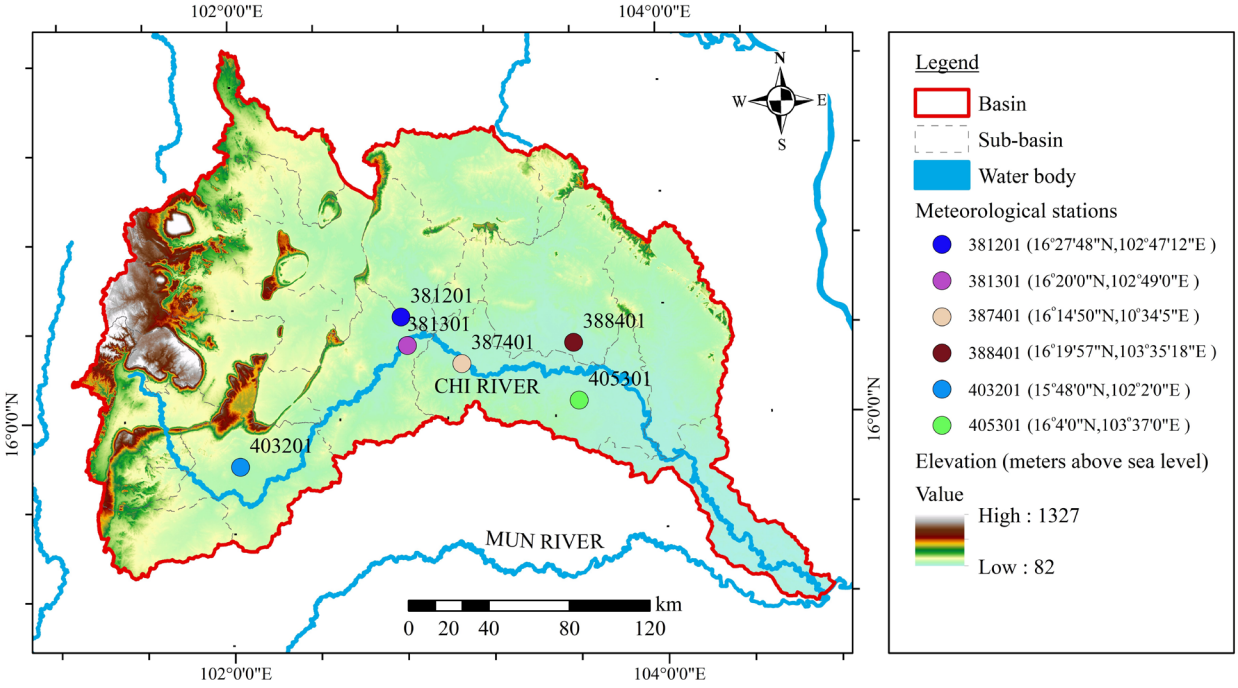

Fig. 2 Location of study area in Chi River Basin, northeastern Thailand.

The first step involved bias correction and projection methods using climatic parameters (daily rainfall, maximum and minimum temperatures) for the periods 1970–2010 (historical) and 2011−2100 (future), by applying a linear regression formula. The future time steps were delineated into three periods: the 2020s (2011–2040); the 2050s (2041–2070); and the 2080s (2071–2100). Second, future monthly precipitation data from the climate change projection method was used to simulate the SPI, generated using RStudio version 4.4.0 (http://www.R-project.org/), an integrated development environment for R, a programming language for statistical computing and graphics (R Core Team, 2024). Third, the SPEI values were derived from future monthly rainfall and maximum and minimum temperatures under the RCP4.5 and RCP8.5 scenarios. Monthly SPEI values were simulated using a standard R-package in the RStudio software for both the SPI and SPEI indices (Vicente-Serrano et al., 2010; Cadro and Uzunovic, 2013; Janecka et al., 2022). Fourth, future SPI and SPEI values were compared at the six meteorological stations located in the CRB. Drought durations of 1 mth, 3 mth and 6 mth, corresponding to drought hazard impacts on rice, field crops (cassava, maize, sugarcane) and orchards or perennial crops (coconut, longan, mango, rubber tree), respectively. The trends and differences in the two drought indices (SPI and SPEI) under the RCP4.5 and RCP8.5 scenarios were determined based on Pearson's correlation coefficient values. For validation purposes, statistical parameters —the coefficient of determination (R^2), Nash-Sutcliffe efficiency (NSE), percent bias (PBIAS) and mean absolute error (MAE)—were used to compare simulated SPI and SPEI data under the RCP4.5 and RCP8.5 scenarios with observed data from 2011−2020.

Climate change projection

Bias correction is a common technique used to compare and correct simulated and observed climatic data to enhance the accuracy of simulated climate data (Shrestha et al., 2016). The linear scaling formula calculates corrected simulation data from actual simulation data, adjusted by a monthly constant. However, the simulated climate parameters from ACCESS, CNRM and MPI are still inaccurate for use in the climate change projection method and need correction using the linear scaling formula for rainfall (Equations 1 and 2) and temperature (Equations 3 and 4), according to Promping and Tingsanchali (2020). Equations 1 and 2 correct rainfall from simulated RCM data by multiplying by a monthly constant, calculated from the observed daily rainfall divided by the simulated daily rainfall for each RCM and then averaged over the number of days per month, which converts the data from daily to monthly units. Equations 3 and 4 are correction formulas for the maximum and minimum temperatures, calculating the corrected simulated temperature from the simulated temperature plus a monthly constant, generated from the observed daily temperature minus the simulated daily temperature and averaged over the number of days per month, ensuring consistency throughout the time scale. These equations were separated into two time steps: historical (1970−2010) and simulated RCM data (2011−2100), as shown in Equations 1 and 3 and Equations 2 and 4, respectively. All corrected simulated climatic data from the three RCMs was checked for performance and accuracy using a sensitivity performance index, namely the mean and ± SD, to measure the dispersion and central tendency of the corrected climatic data.

Rainfall correction Equations:

$$R'_{his,d} = R_{his,d} \cdot Xm \; ; \; Xm = [R_{obs,d}/R_{his,d}]/n_d \quad (1)$$

$$R'_{sim,d} = R_{sim,d} \cdot Xm \quad (2)$$

Maximum and minimum temperature correction Equations:

$$T'_{his,d} = T_{his,d} + Ym \; ; \; Ym = [T_{obs,d} - T_{his,d}]/n_d \quad (3)$$

$$T'_{sim,d} = T_{sim,d} + Ym \quad (4)$$

where, R is the rainfall, T is the temperature (measured in degrees Celsius, d is the daily unit, m is the monthly unit, ' is the corrected value, n_d is the number days in the month, obs is the observed data during 1970−2010, X and Y are monthly constants for rainfall and temperature and his and sim are historical and simulated RCM data during 1970−2010 and 2011−2100, respectively.

Investigation of standardized precipitation index

The SPI is a relative drought index that is simple to use for presenting drought hazard, intensity, duration and severity, based on precipitation rates (McKee et al., 1993; Svoboda and Fuchs, 2016). This study used simulated climate data from three RCMs (rainfall) to simulate SPI1 for a 1 mth drought duration, reflecting the drought hazard impact on rice,

assuming this crop can withstand up to 1 mth without rainfall. SPI3 was used for a 3 mth drought duration to assess the impact on field crops (cassava, maize, sugarcane) and SPI6 was used for a 6 mth drought duration to evaluate the impact on orchard crops (Foyhirun and Promping, 2021). The SPI was calculated using monthly average rainfall data from three RCMs for 1980-2010 (past) and 2011–2100 (future). The future time steps were divided into three periods: the 2020s (2011−2040); the 2050s (2041−2070); and the 2080s (2071−2100).

The observed and simulated daily rainfall data were converted to monthly rainfall rates for January–December. The gamma distribution function is typically used for monthly rainfall distribution for SPI values and needs to be converted to a standard normal distribution for monthly rainfall, as suggested by Thom (1996) and Shah et al. (2015). After conversion to a normal distribution, the monthly rainfall was calculated as SPI values using Equation 5, which typically ranges from -3 to 3, depending on the monthly rainfall rate. All methods for generating SPI could be applied using the RStudio and R integrated software packages.

The standardized precipitation index (SPI) is provided by Equation 5:

$$SPI = (X_i - \bar{X})/\mathrm{SD} \quad (5)$$

where is the normalized monthly precipitation, is the long-term average monthly precipitation (measured in millimeters) and SD is the standard deviation.

Standardized precipitation evapotranspiration index

The SPEI is an extension of the SPI that requires additional climatic data on precipitation and potential evapotranspiration (PET). The computed SPEI value was calculated using Equation 6 and then input into Equation 5, following the original SPI calculation method. However, the SPEI can also refer to the impact of climate drought on water resources (Beguería et al., 2013):

$$D_M = Pr_M - PET_M \quad (6)$$

where D is a simple measurement of the water deficits or surpluses aggregated, PET is the potential evapotranspiration (measured in millimeters per day), Pr is the precipitation (measured in millimeters) and M is the monthly unit.

Potential evapotranspiration (PET, measured in millimeters per day) was determined using the Hargreaves method (Hargreaves and Allen, 2003) which is appropriate for studies where only temperature data are available. The Hargreaves-Samani equation is given as Equation 7:

$$PET = 0.0023\,(T_{max} - T_{min})^{0.5}\,(T_{mean} + 17.8)R_a \quad (7)$$

where T_{max}, T_{min}, T_{mean} are the maximum, minimum and mean temperatures (measured in degrees Celsius), respectively, R_a is the extraterrestrial radiation (in millimeters per day) using Equation 8, which is a function of latitude and the month of the year.

$$R_a = [24(60)/\pi]G_{sc}d_r[\omega_s \sin(\varphi) \sin(\delta) + \cos(\varphi) \cos(\delta) \sin(\omega_s)] \quad (8)$$

where G_{sc} is the solar constant (0.0820/MJm^2/min), d_r is the inverse relative Earth-Sun distance, ω_s is the sunset hour angle (rad), φ is the latitude (rad) and δ is the solar declination (rad). The extraterrestrial radiation (R_a) can be converted to millimeters per day by multiplying by 0.408 (Allen et al., 1998).

The SPEI in this study was calculated using monthly average simulated rainfall and maximum and minimum temperatures from three RCMs. Three time scales were analyzed: SPEI1 for rice, SPEI3 for field crops and SPEI6 for orchards/perennials. The SPEI was presented in three time steps: the 2020s, 2050s and 2080s under two representative concentration pathways (RCP4.5 and RCP8.5).

Interrelationship between standardized precipitation index and standardized precipitation evapotranspiration index

Drought, unlike flooding, has a high likelihood of occurring every summer season. It directly affects various hydrological processes such as precipitation, runoff, evapotranspiration and infiltration. The comparative analysis of the SPI and SPEI was conducted using Pearson's correlation coefficient (*r*), according to Tefera et al. (2019) and Ojha et al. (2021). Pearson's correlation coefficient, ranging from -1 to 1, is a straightforward statistical parameter used to calculate and measure the relationship between two datasets, indicating a total negative or positive linear correlation, respectively.

Performance and verification of drought indexes

The past drought indices (SPI and SPEI) were validated using statistical performance parameters—R^2 and NSE (Nash and Sutcliffe, 1970; Walz et al., 2015; Asare-Kyei et al., 2017). R^2 is a measure frequently used in regression analysis, but it has its limitations as it only evaluates the linear relationship between observed and simulated values (Legates and McCabe, 1999). An R^2 value close to 1 is considered very good. An NSE efficiency of 1 signifies a perfect match between the simulated and observed data, while an NSE efficiency of 0 indicates that the model's simulations are as accurate as the mean of the observed data (Gebre, 2015; Cardoso de Salis et al., 2019). MAE (Rashid and Beecham, 2019; Yalçın et al., 2023) and PBIAS (Nouri, 2023) have been used widely in evaluating the accuracy and central tendency of model performance. MAE measures the average absolute difference between the simulated and observed values (Wang and Lu, 2017), while PBIAS measures the average tendency of the simulated values to be larger or smaller than the observed ones (Gupta et al., 1999; Moriasi et al., 2007).

Results and Discussion

Evaluated climate change projection

The projection of future climate change was analyzed using three regional climate models (ACCESS, CNRM and MPI) under the RCP4.5 and RCP8.5 scenarios by applying bias regression methods. Climate data from six meteorological stations (381201, 381301, 387401, 388401, 403201 and 405301) were collected from the TMD and RID (Fig. 2). The climate change projection method applied linear downscaling formulas, as shown in Equations 1−2 (for rainfall) and 3-4 (for temperature), to compare and correct the simulated climate data from past and future time steps. Additionally, statistical performance indexes (standard deviation and mean) were analyzed to recheck the similarity level of both observed and simulated climate data during the historical decade (Table 1).

The statistical performance of the corrected simulation and observation including rainfall and maximum and minimum temperatures, is shown in terms of mean and ± SD values for each meteorological station. The mean and SD refer to the dispersion and central tendency of ACCESS, CNRM and MPI compared to the historical data (1970–2010). Table 1 shows that both the mean and SD of rainfall, maximum and minimum temperatures from MPI were more similar to historical values than those from ACCESS and CNRM. However, stations 381201, 381301, 387401 and 388401 had lower rainfall dispersion levels for all RCMs than the historical period. The mean and SD values of maximum and minimum temperature tended to have similar levels for all stations. Overall, the performance of the climate change projection could be used to predict future rainfall, maximum and minimum temperatures under three RCMs with different RCPs.

Table 1 Performance of downscaling method (ACCESS-CSIRO-CCAM, CNRM-CM5-CSIRO-CCAM, MPI-ESM-CSIRO-CCAM)

Station	381201		381301		387401		388401		403201		405301	
ID	Mean	SD	Mean	SD	Mean	SD	Mean	SD	Mean	SD	Mean	SD
						Rainfall (mm)						
Historical	3.41	10.51	3.20	10.54	3.73	11.46	4.00	12.69	3.02	9.54	3.59	11.11
ACCESS	3.62	7.22	3.31	7.52	3.86	7.71	4.36	7.60	3.22	8.16	3.88	10.99
CNRM	3.51	7.63	3.38	7.16	3.72	7.29	4.38	8.99	3.07	7.44	3.65	12.21
MPI	2.95	5.78	3.12	6.13	3.58	6.88	4.01	8.52	2.96	7.98	3.63	10.92
						Maximum temperature (°C)						
Historical	32.57	3.11	32.45	3.11	32.02	3.01	32.27	2.99	32.60	3.08	32.18	3.05
ACCESS	32.06	3.42	32.02	3.41	31.53	3.41	31.90	3.94	31.62	3.49	30.41	3.63
CNRM	31.72	3.29	31.85	3.50	31.53	3.41	32.80	4.32	31.82	3.39	30.80	3.51
MPI	32.24	3.35	32.02	3.39	31.52	3.11	32.07	3.25	31.99	3.28	30.32	3.88
						Minimum temperature (°C)						
Historical	22.13	3.54	21.80	3.76	22.27	3.64	22.12	3.56	22.53	3.03	22.13	3.67
ACCESS	21.72	3.66	21.55	3.61	21.91	3.74	21.92	3.63	22.07	3.27	21.61	3.74
CNRM	20.85	3.91	21.38	3.87	21.91	3.80	22.76	3.64	22.16	3.29	21.98	3.57
MPI	21.90	3.51	21.54	3.67	21.55	3.52	21.78	3.50	22.32	3.11	21.60	3.75

ACCESS-CSIRO-CCAM, CNRM-CM5-CSIRO-CCAM and MPI-ESM-LR-CSIRO-CCAM = three different regional climate models used to simulate future climate change projections: (from the Collaboration for Australian Weather and Climate Research, the National Centre for Meteorological Research and the European Network of Earth System Modelling, respectively)

The climate change projection was analyzed until the twenty-first century and separated into three time steps: the 2020s (2011–2040), the 2050s (2041–2070) and the 2080s (2071–2100), used to represent near-term, mid-term and long-term periods. The annual rainfall and maximum and minimum temperatures at the Khon Kaen Meteorological Station, Khon Kaen province, Thailand, located in the middle part of CRB, show a fluctuating trend in annual rainfall and a slight increase in both maximum and minimum temperatures (Fig. 3). The historical annual rainfall and maximum and minimum temperatures were 1,241 mm, 32.83°C and 22.34°C, respectively. The annual rainfall changed slightly from 1,241 mm to 1,235 mm (RCP4.5) and from 1,258 mm to 1,301 mm (RCP8.5) during the 2020s to the 2080s, respectively. The maximum temperature for both RCPs increased from 33.12°C to 34.44°C or +1.32°C (RCP4.5) and from 33.31°C to 36.04°C or +2.73°C (RCP8.5) from the 2020s to the 2080s. Additionally, the minimum temperature increased from 22.62°C to 23.82°C or +1.20°C (RCP4.5) and from 22.76°C to 25.52°C or +2.76°C (RCP8.5).

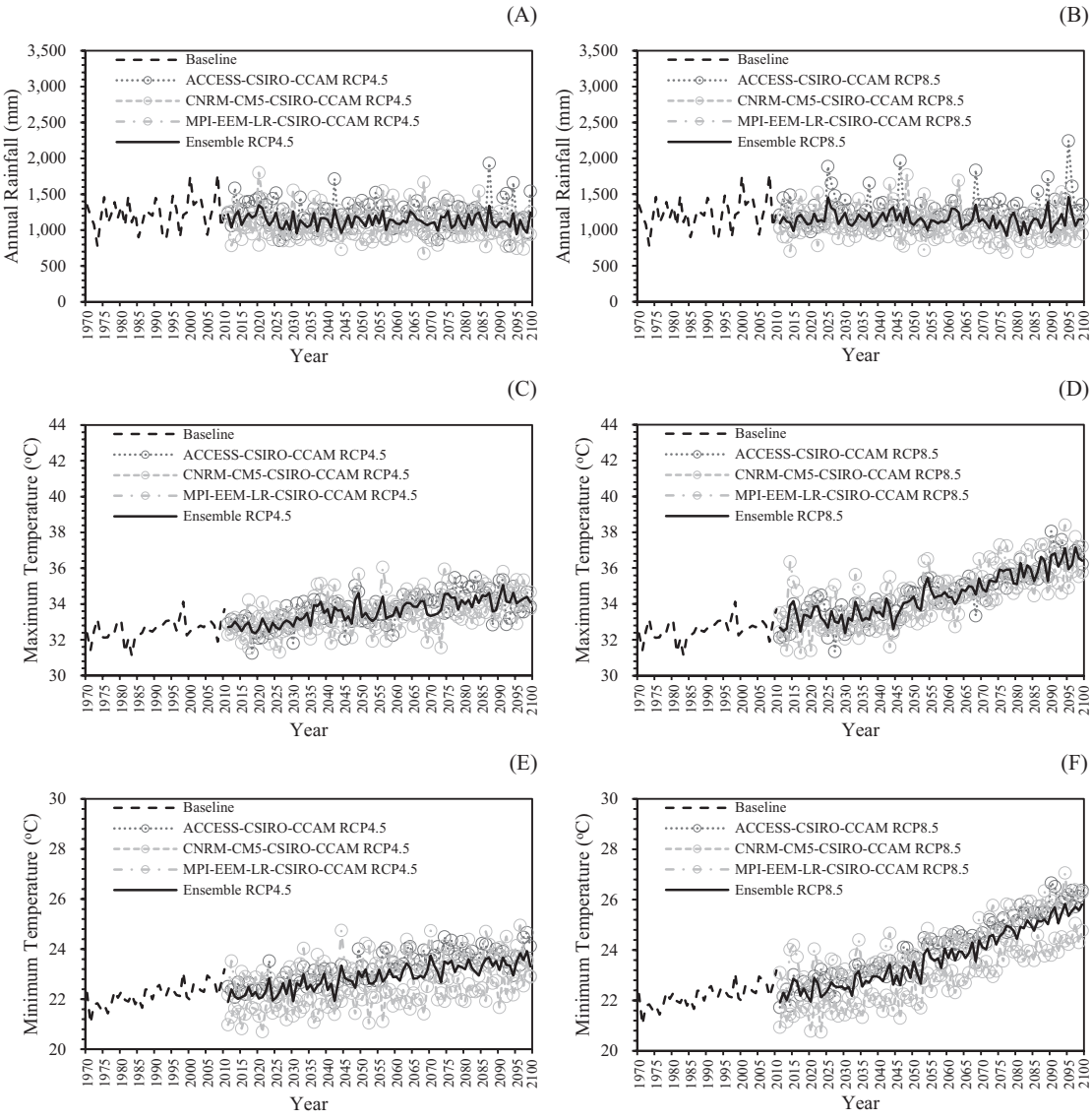

Fig. 3 Annual rainfall and maximum and minimum temperatures at Khon Kaen Meteorological Station (381201) under two commonly used climate change representative concentration pathways from 1970 to 2100: (A, C, E) RCP4.5; (B, D, F) RCP8.5 , where ACCESS-CSIRO-CCAM, CNRM-CM5-CSIRO-CCAM and MPI-ESM-LR-CSIRO-CCAM = three different regional climate models used to simulate future climate change projections: (from the Collaboration for Australian Weather and Climate Research, the National Centre for Meteorological Research and the European Network of Earth System Modelling, respectively)

Standardized precipitation index

The projected monthly rainfall was used to generate SPI values using Equation 5 with three time steps from the 1990s to the 2020s, 2050s and 2080s, with RCP4.5 and RCP8.5. The six meteorological stations located in the CRB had different drought hazard levels depending on the drought duration (1 mth, 3 mth and 6 mth). The results of the SPI value from the investigated SPI generation method are presented in Table 2. The range of SPI values normally varies between -3 and 3, with the SPI values tending to change from negative (near-term) to positive (mid-term) and then back to negative (long-term) for the three case studies (SPI1, SPI3 and SPI6). However, during the 2020s, all values were near zero, indicating a mild drought level. SPI6 tended to have a higher drought hazard level than SPI3 and SPI1, respectively.

Standardized precipitation evapotranspiration index

The climate change projection estimated future monthly rainfall and maximum and minimum temperatures that were used to calculate the SPEI. Both the average monthly maximum and minimum temperatures were evaluated for evapotranspiration (PET), using Equations 7–8, which was used to evaluate the SPEI values as input to Equation 6. All trends of the SPEI from the six meteorological stations showed a similar change from positive to negative values during the 2020s and 2080s, indicating a change from wet to drought levels in the future (Table 2). Additionally, the drought hazard level in SPEI6 had higher negative values than SPEI3 and SPEI1, respectively. The drought duration in SPEI6 had a longer water shortage period with RCP8.5 than with RCP4.5. The gap differences between RCP4.5 and RCP8.5 was widely observed in the monthly rainfall and maximum and minimum temperatures.

Comparison of standardized precipitation index and standardized precipitation evapotranspiration index

In terms of temporal analysis, the SPI values showed similar trends and results to those analyzed from only the monthly rainfall data. However, unlike the SPI values, the SPEI values required input data from monthly rainfall and maximum and minimum temperatures. Both these temperature values had a greater effect on the SPEI trend,

Table 2 Standardized precipitation index (SPI) and standardized precipitation evapotranspiration index (SPEI) values for different monthly values at six meteorological stations for different modelled periods

Station number	1990s		2020s				2050s				2080s			
			RCP4.5		RCP8.5		RCP4.5		RCP8.5		RCP4.5		RCP8.5	
	SPI1	SPEI1	SPI1	SPEI1	SPI1	SPEI1	SPI1	SPEI1	SPI1	SPEI1	SPI1	SPEI1	SPI1	SPEI1
381201	0.14	0.03	-0.06	0.10	-0.08	0.17	0.04	0.04	0.07	0.06	0.09	-0.08	0.00	-0.25
381301	0.14	0.01	-0.06	0.12	-0.07	0.18	0.03	0.03	0.07	0.05	0.08	-0.09	0.01	-0.26
387401	0.12	0.01	-0.06	0.07	-0.10	0.17	0.12	0.09	0.09	0.06	-0.02	-0.15	0.04	-0.25
388401	0.03	0.01	-0.05	0.12	-0.06	0.17	0.04	0.04	0.08	0.06	0.03	-0.15	0.02	-0.26
403201	0.14	0.02	-0.08	0.12	-0.06	0.21	0.03	0.04	0.06	0.03	0.11	-0.12	0.02	-0.26
405301	0.11	0.00	-0.08	0.07	-0.07	0.11	0.07	0.04	0.08	0.08	0.05	-0.10	0.02	-0.21
	SPI3	SPEI3	SPI3	SPEI3	SPI3	SPEI3	SPI3	SPEI3	SPI3	SPEI3	SPI3	SPEI3	SPI3	SPEI3
381201	0.00	0.00	-0.06	0.11	-0.09	0.20	0.02	0.03	0.12	0.11	0.13	-0.07	-0.10	-0.40
381301	0.00	0.00	-0.05	0.11	-0.09	0.20	0.03	0.04	0.12	0.11	0.10	-0.09	-0.10	-0.40
387401	0.01	0.00	-0.09	0.06	-0.13	0.20	0.13	0.11	0.14	0.11	-0.07	-0.21	-0.02	-0.40
388401	0.02	0.01	-0.1	0.09	-0.04	0.20	0.08	0.06	0.1	0.11	0.01	-0.14	-0.12	-0.39
403201	0.00	0.00	-0.08	0.11	-0.07	0.22	0.03	0.04	0.09	0.08	0.13	-0.09	-0.05	-0.35
405301	-0.01	-0.01	-0.12	0.02	-0.09	0.12	0.09	0.06	0.14	0.14	0.06	-0.08	-0.11	-0.34
	SPI6	SPEI6	SPI6	SPEI6	SPI6	SPEI6	SPI6	SPEI6	SPI6	SPEI6	SPI3	SPEI6	SPI6	SPEI6
381201	-0.02	-0.01	-0.04	0.12	-0.04	0.26	0.03	0.04	0.13	0.14	0.13	-0.07	-0.26	-0.54
381301	-0.02	-0.01	-0.04	0.12	-0.04	0.25	0.05	0.06	0.14	0.15	0.10	-0.09	-0.25	-0.53
387401	-0.02	-0.01	-0.06	0.11	-0.12	0.26	0.14	0.13	0.17	0.14	-0.12	-0.28	-0.11	-0.54
388401	0.02	0.02	-0.05	0.10	0.04	0.27	0.09	0.10	0.13	0.14	-0.06	-0.19	-0.28	-0.53
403201	-0.01	0.00	-0.07	0.09	-0.05	0.25	0.04	0.06	0.10	0.10	0.13	-0.06	-0.14	-0.42
405301	-0.01	0.00	-0.10	0.04	-0.01	0.19	0.11	0.08	0.16	0.18	0.00	-0.14	-0.27	-0.49

Numeral in SPI and SPEI terms indicates monthly drought duration modelled, where 1 = 1 mth, 3 = 3 mth and 6 = 6 mth.

resulting in different gaps in the simulated values for the SPI and SPEI (Fig. 4). The difference in gaps tended to change from widely negative (in the 2020s) to near zero (in the 2050s) and widely positive (in the 2080s) for the three SPIs under RCP4.5 and RCP8.5. This indicated that both the SPI and SPEI values were very different during the 2020s and 2080s but were similar during the 2050s. The drought interval based on the 6 mth period generally had a longer water shortage duration with similar fluctuation dynamic trends as in the 1 mth and 3 mth drought intervals. RCP4.5 had lower levels of positive and negative fluctuations and longer drought duration gaps compared to RCP8.5, similar to the drought duration intervals.

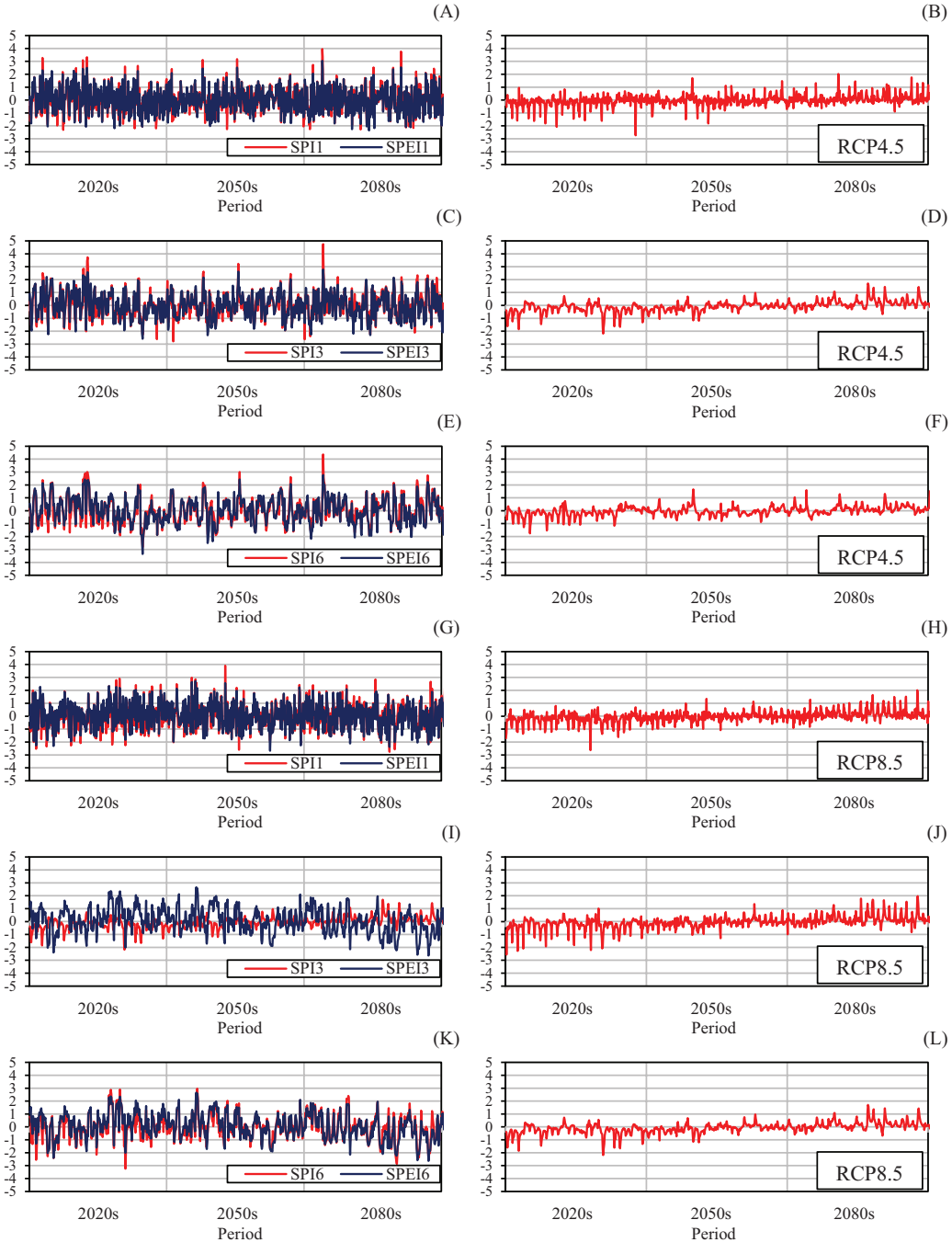

Fig. 4 Temporal evolution during 2020s, 2050s and 2080s (A, C, E, G, I, K) and their differences (B, D, F, H, J, L) for standardized precipitation index (SPI) and standardized precipitation evapotranspiration index (SPEI) values using climate change representative concentration pathways (RCP4.5 and RCP8.5), where numeral in SPI and SPEI terms indicates monthly drought duration modelled for 1 = 1 mth, 3 = 3 mth and 6 = 6 mth at Khon Kaen Meteorological Station (381201) in the Chi River Basin

The difference between the SPI and the SPEI at Khon Kaen Meteorological Station, located in the middle part of the CRB, was analyzed for three time periods (the 2020s, the 2050s and the 2080s). There were relatively small differences during the 1990s period, with values of approximately 0.11, 0.00 and -0.01 for SPI1 and SPEI1, for SPI3 and SPEI3 and for SPI6 and SPEI6, respectively. Under RCP4.5, the differences were approximately -0.15, -0.16 and -0.14 in the 2020s; 0.00, -0.01 and -0.01 in the 2050s; and 0.17, 0.20 and 0.19 in the 2080s for SPI1 and SPEI1, for SPI3 and SPEI3 and for SPI6 and SPEI6, respectively. Similarly, under RCP8.5, the corresponding differences were -0.23, -0.29 and -0.30 in the 2020s; 0.02, 0.00 and -0.01 in the 2050s and 0.25, 0.30 and 0.28 in the 2080s. These values indicated that the SPEI had higher values than SPI in the 2020s, as reflected by the negative differences. In the 2050s, the SPI and SPEI values were nearly equal, with differences close to zero. In contrast, the SPI values exceeded SPEI values in the 2080s, as shown by the positive differences.

The correlation analysis between the SPI and the SPEI at different time scales at the Khon Kaen Meteorological Station (381201) indicated strong positive linear correlations for both past data (the 1990s) and projected data (the 2020s, 2050s and 2080s). The Pearson's correlation coefficient (r), which measures the relationship between two variables (based on values in the range from -1 to 1), was used in this analysis. This correlation coefficient was very high between SPI and SPEI for the 1990s period (r = 0.89, 0.97 and 0.97 at significance levels of 0.01, 0.05 and 0.05, respectively, for the 1 mth, 3 mth and 6 mth timescales, respectively) or near-perfect (Fig. 5). The correlation values for RCP4.5 and RCP8.5 were: in the 2020s,

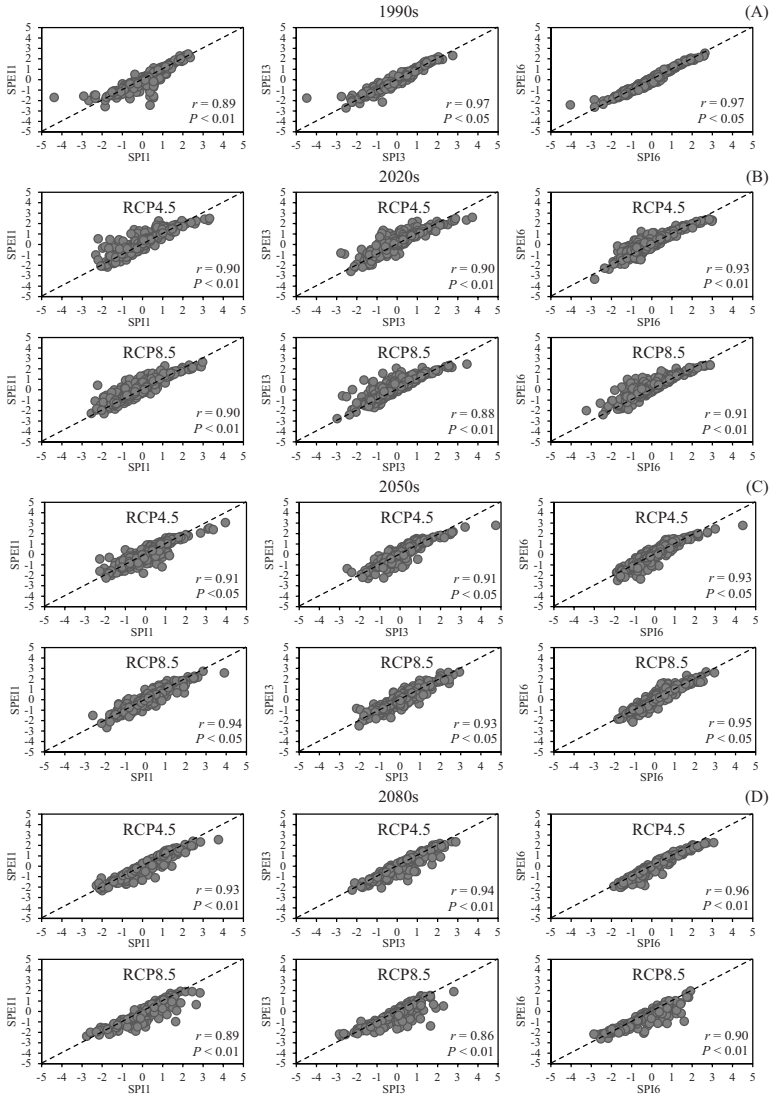

Fig. 5 Pearson correlation coefficients at Khon Kaen Meteorological Station (381201) for different modelling periods using standardized precipitation index (SPI) and standardized precipitation evapotranspiration index (SPEI) values: (A) 1990s; (B) 2020s; (C) 2050s; (D) 2080s, where numeral in SPI and SPEI terms indicates monthly drought duration modelled for 1 = 1 mth, 3 = 3 mth and 6 = 6 mth.

r = 0.90 and 0.90, respectively; in the 2050s, r = 0.91 and r = 0.94, respectively; and in the 2080s, r = 0.93 and r = 0.89, respectively. For the 3 mth duration, the correlation values for SPI3 and SPEI3 were: in the 2020s, r = 0.90 and 0.88, respectively; in the 2050s, r = 0.91 and r = 0.93, respectively; and in the 2080s, r = 0.94 and r = 0.86, respectively. For the 6 mth duration, the linear correlations for SPI6 with SPEI6 were in the ranges r = 0.93–0.96 (RCP4.5) and 0.90–0.95 (RCP8.5) during the 2020–2080 period. All correlation values for SPI and SPEI with the different drought durations were in the range r = 0.86–0.96 and were significant at the 0.01 and 0.05 levels for both RCP4.5 and RCP8.5 (2-tailed test), indicating strong positive correlations between the two indices for both past and future periods.

The SPI and SPEI values were simulated and mapped using the inverse distance weighted technique, as described by Bagheri (2016) and Kuntiyawichai and Wongsasri (2021). These values were assessed from monthly values during the dry seasons (November–April) from 2011 to 2020 (Fig. 6). The drought intervals of 1 mth, 3 mth and 6 mth corresponded to the drought situations for rice, field crops and orchards/perennials, respectively. The simulated SPI1 maps under both RCP4.5 and RCP8.5 indicated potential drought events across all paddy field areas. For RCP4.5, SPEI1 tended to show unaffected drought areas, while for RCP8.5, it showed a mix of affected areas and areas not affected by drought. For field crop lands, SPEI3 under RCP4.5 indicated unaffected or wet conditions. SPI3 under RCP4.5 and SPEI3 under RCP8.5 showed one-half of the area as dry, while the other half was not affected by drought. However, SPI3 under RCP8.5 indicated completely dry conditions across all areas. For orchards/perennials, SPEI6 under both RCP4.5 and RCP8.5 showed only unaffected or wet conditions, except for SPI6 under RCP8.5 which indicated drought conditions. In summary, the SPI1, SPI3 and SPI6 maps under RCP8.5 mostly showed agricultural areas affected by dry conditions. In contrast, these same maps under RCP4.5 mostly showed unaffected or wet conditions.

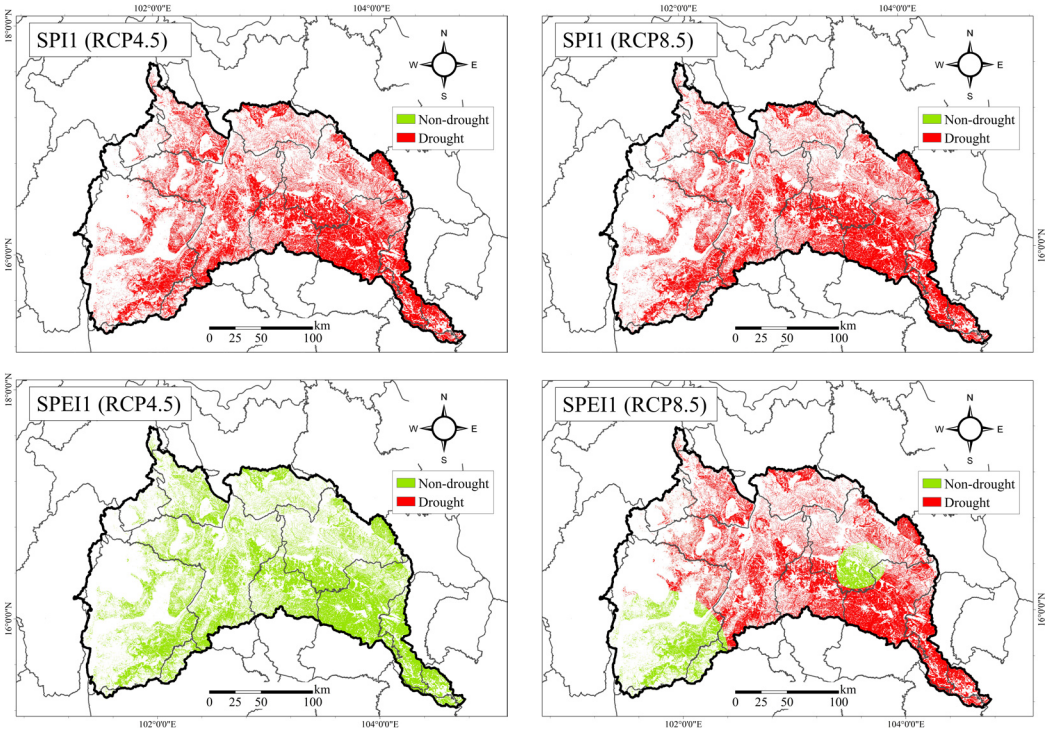

(A) 1 mth drought duration for paddy field areas

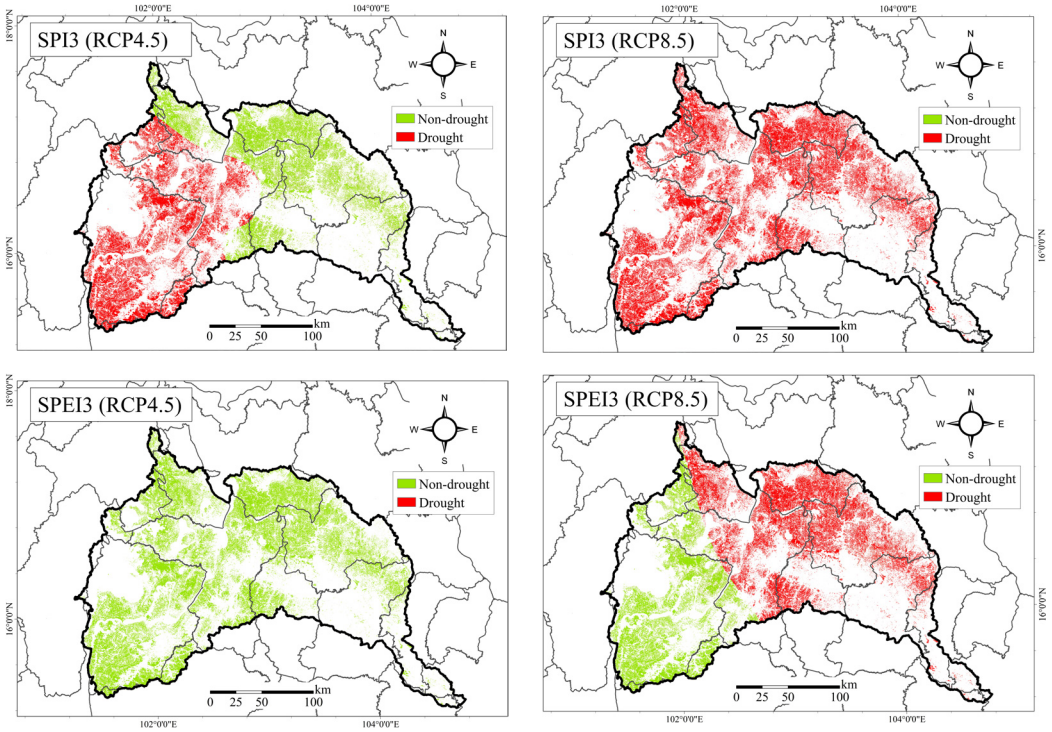

(B) 3 mth drought duration for field crop areas

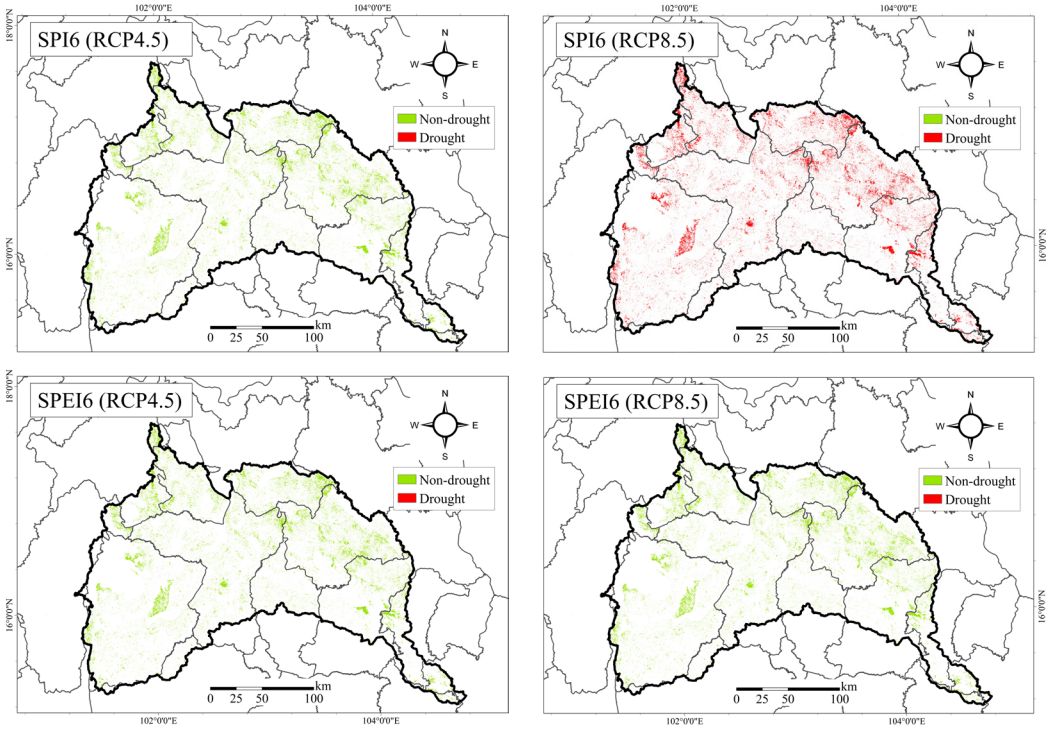

(C) 6 mth drought duration for orchards/perennials areas

Fig. 6 Spatial distribution maps of drought/non-drought maps using standardized precipitation index (SPI) and standardized precipitation evapotranspiration index (SPEI) values with climate change representative concentration pathways (RCP4.5 and RCP8.5) during 2011-2020: (A) 1 mth drought duration for paddy field areas; (B) 3 mth drought duration for field crop areas; (C) 6 mth drought duration for orchards/perennials areas, where numeral in SPI and SPEI terms indicates monthly drought duration modelled for 1 = 1 mth, 3 = 3 mth and 6 = 6 mth

The areas affected and unaffected by drought during 2011−2020 were categorized into three types based on the duration of the drought (1 mth, 3 mth and 6 mth), as shown in Table 3. These areas were simulated under two representative concentration pathways (RCP4.5 and RCP8.5). Under RCP4.5, the areas affected by drought for durations of 1 mth, 3 mth and 6 mth based on the SPI were 15,182 km², 6,485 km² and 0 km², respectively. For RCP8.5, the corresponding areas were 15,182 km², 12,803 km² and 2,957 km², respectively. The unaffected areas under RCP4.5 for 3 mth and 6 mth based on the SPI were 6,318 km² and 2,957 km², respectively. Based on the SPEI, under RCP4.5, all of these areas were classified as non-drought. The unaffected areas for drought durations of 1 mth, 3 mth and 6 mth were 2,906 km², 5,424 km² and 2,957 km², respectively, under RCP8.5. For SPEI under RCP8.5, the affected areas for drought durations of 1 mth and 3 mth were 12,276 km² and 7,379 km², respectively. In other words, the SPI has had a great impact on drought events over the past decade in most agricultural areas. This impact was greater than that of the SPEI, particularly in detecting drought severity in regions classified as unaffected by drought. This trend has also been observed in several parts of the world, such as Burkina Faso (Bontogho et al., 2023), Chile (Meseguer-Ruiz et al., 2024), Indonesia (Suroso et al., 2021) and Zambia (Tirivarombo et al., 2018), where the SPI has consistently produced higher drought severity estimates compared to the SPEI.

The model performance was evaluated using R^2, NSE, PBIAS and MAE to verify and compare the simulated and observed drought areas. This comparison was done using location-by-location techniques (Table 4). The observed data involved 434 locations for affected areas and 263 locations for unaffected areas. For the SPI under RCP4.5, 547 locations were affected and 150 locations were unaffected. Under RCP8.5, all 697 locations were clearly affected. For the SPEI, all 697 locations under RCP4.5 were clearly unaffected, while 493 and 204 locations were affected and unaffected under RCP8.5, respectively. Comparing observed and simulated data, several locations showed consistency and differences. For the SPI values under RCP4.5 and RCP8.5, 418 and 279 locations were consistent, whereas 434 and 263 locations were different. For the SPEI values predicted under RCP4.5 and RCP8.5, 263 and 340 locations were consistent, whereas 434 and 357 locations were different. These results are illustrated in Fig. 7.

The R^2, NSE, RMSE and MAE values for SPI were 0.01, -0.70, 0.16 and 0.40, respectively, for RCP4.5 and 0.00, -0.61, 0.38 and 0.38 for RCP8.5, respectively. For SPEI, based on RCP4.5 and RCP8.5: the R^2 values were 0.00 and 0.02, respectively; the NSE values were -1.65 and -1.18, respectively; the PBIAS values were -0.62 and 0.09, respectively; and the MAE values were 0.62 and 0.51, respectively.

Table 3 Affected and unaffected drought areas (km²) simulated under two representative concentration pathways (RCP4.5 and RCP8.5) during 2011-2020 based on standardized precipitation index (SPI) and standardized precipitation evapotranspiration index (SPEI) data.

RCP	4.5			8.5		
Interval (mth)	1	3	6	1	3	6
SPI						
Non-drought		6,318	2,957			
Drought	15,182	6,485		15,182	12,803	2,957
SPEI						
Non-drought	15,182	12,803	2,957	2,906	5,424	2,957
Drought				12,276	7,379	

Table 4 Performance of standardized precipitation index (SPI) and standardized precipitation evapotranspiration index (SPEI) data under two representative concentration pathways (RCP4.5 and RCP8.5) during 2011-2020.

Parameter	RCP	Number of locations		Comparison		Statistical indicator			
		Affected	Unaffected	Consistent	Different	R^2	NSE	PBIAS	MAE
SPI	4.5	547	150	418	279	0.01	-0.70	0.16	0.40
	8.5	697	0	434	263	0.00	-0.61	0.38	0.38
SPEI	4.5	0	697	263	434	0.00	-1.65	-0.62	0.62
	8.5	493	204	340	357	0.02	-1.18	0.09	0.51

R^2 = coefficient of determination; NSE = Nash-Sutcliffe efficiency; PBIAS = percent bias; MAE = mean absolute error.

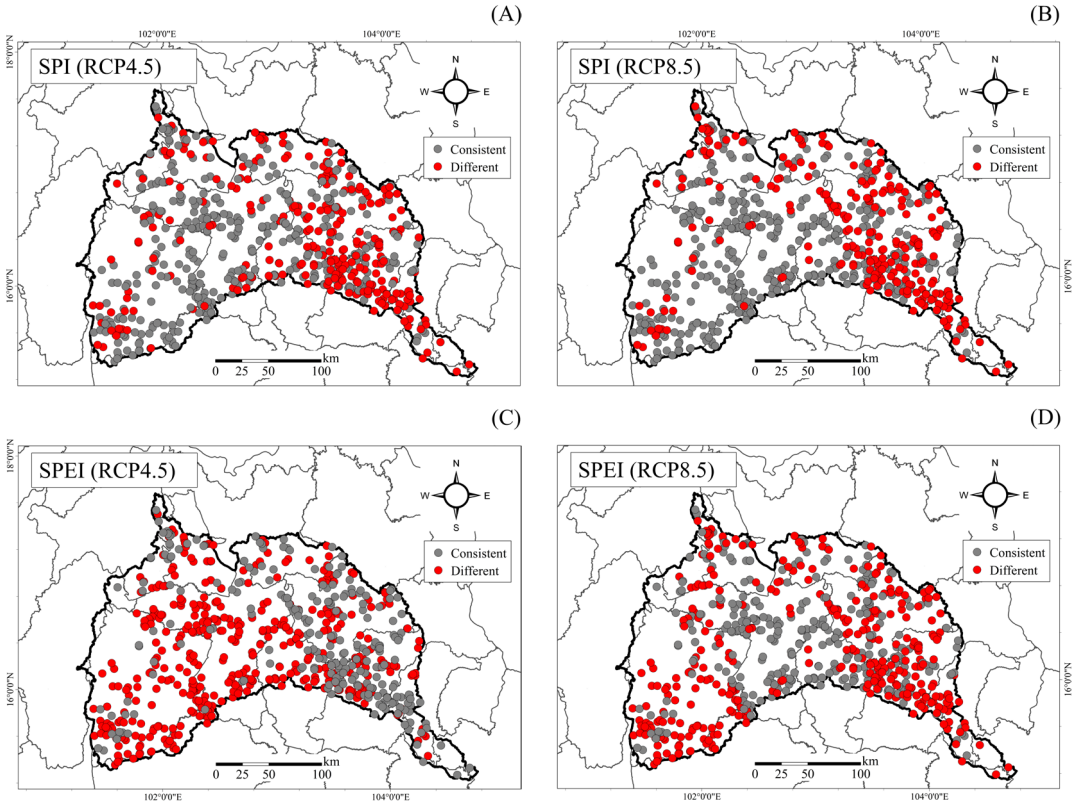

Fig. 7 Differences between simulated values under two representative concentration pathways (RCP4.5 and RCP8.5) during 2011-2020 based on standardized precipitation index (SPI) and standardized precipitation evapotranspiration index (SPEI) data: (A) SPI and RCP4.5; (B) SPI and RCP8.5; (C) SPEI and RCP4.5; (D) SPEI and RCP8.5.

Conclusions

Drought indicators and indices can be widely applied to analyze meteorological, hydrological, moisture content and remote sensing data (WMO and GWP, 2016). The current study focused on the meteorological aspect, as it is straightforward to define drought hazard levels from precipitation, evapotranspiration and temperature. The SPI and SPEI are common meteorological drought parameters that accurately reflect the impact of shortages on agricultural areas (Pathak and Dodamani, 2019; Öz et al., 2024). The aim of the current study was to compare predicted drought indices based on climate change projections under two representative concentration pathways.

Based on the current results, projected future climate change will alter rainfall from 1,241 mm to 1,235 mm under RCP4.5 and from 1,258 mm to 1,301 mm under RCP8.5 during the simulated periods from the 2020s (2011−2040) to the 2080s (2071−2100). The maximum and minimum temperatures for both RCPs were projected to increase from 33.12°C to 34.44°C and from 22.62°C to 23.82°C under RCP4.5 and from 33.31°C to 36.04°C and from 22.76°C to 25.52°C under RCP8.5 from the 2020s until the 2080s. The SPI values were projected to change from negative (dry conditions) in the 2020s to positive (wet conditions) in the 2050s and back to negative (dry conditions) in the 2080s. The SPEI values showed a different trend from the SPI, changing from positive (wet conditions) in the 1990s, 2020s and 2050s, to negative (dry conditions) in the 2080s. The highest drought values for both SPI and SPEI were for SPI6/SPEI6, which were higher than for SPI3/SPEI3 and SPI1/SPEI1, respectively. The difference between these indices was wide during the 1990s, 2020s and 2080s and narrowed during the 2050s. The linear correlation analysis between SPI and SPEI at different time scales at Khon Kaen Meteorological Station (381201) with the 1990s, 2020s, 2050s and 2080s data was in the range 0.86–0.97, indicating a strong positive correlation between the two indices for both past and future periods. The results indicated that the SPI and SPEI produced similar trends and values in the CRB, for both past data and projected periods. However, the linear correlation analysis also suggested

that the SPI could be used as a substitute for the SPEI across all time scales, given that the two indices had a certain degree of agreement. This was consistent with other studies that compared the SPI and SPEI in the Euphrates basin, Turkey (Katipoğlu et al., 2020) and in the Tigray region, Northern Ethiopia (Tefera et al., 2019). Therefore, if there were a lack of temperature data or suitable tools for conducting an SPEI analysis, it would be reasonable to conclude that the SPI could be effectively used to evaluate drought conditions at all investigated time scales in this study area.

The SPI simulations under RCP8.5 suggested potential drought events or dry conditions across all agricultural areas. However, the SPI under RCP4.5 and the SPEI under RCP8.5 presented a combination of areas affected and unaffected by drought. The SPEI under RCP4.5 indicated areas unaffected or experiencing wet conditions. In summary, over the past decade, the SPI and SPEI have had a minimal impact on predicting drought events in most agricultural areas. The model performance approach used revealed that the SPI and SPEI did not align well with observed data, resulting in an unsatisfactory performance rating. Notably, neither the SPI nor SPEI could serve as a standalone drought hazard indicator for the CRB. This was consistent with the 2016 recommendation from World Meteorological Organization and Global Water Partnership (2016), which stated that no single indicator could represent all types of drought (hydrological, agricultural and socioeconomic). The approach applied in the current study should provide valuable guidance for drought assessment in other regions of Thailand.

Conflict of Interest

The authors declare that there are no conflicts of interest.

Acknowledgements

The Thai Meteorological Department and the Royal Irrigation Department, Thailand provided meteorological data.

References

Allen, R.G., Pereira, L.S., Raes, D., Smith, M. 1998. Crop Evapotranspiration: Guidelines for Computing Crop Water Requirements. FAO Irrigation and Drainage Paper 56. FAO, Rome, Italy.

Asare-Kyei, D., Renaud, F.G., Kloos, J., Walz, Y., Rhyner, J. 2017. Development and validation of risk profiles of West African rural communities facing multiple natural hazards. PLOS OneNE. 12: e0171921. doi.org/10.1371/journal.pone.0171921

Bagheri, F. 2016. Mapping drought hazard using SPI index and GIS (a case study: Fars province, Iran). Int. J. Environ. Geoinformatics. 3: 22–28. doi.org/10.30897/ijegeo.285588

Beguería, S., Vicente-Serrano, S.M., Reig, F., Latorre, B. 2013. Standardized precipitation evapotranspiration index (SPEI) revisited: Parameter fitting, evapotranspiration models, tools, datasets and drought monitoring. Int. J. Climatol. 34: 3001–3023. doi.org/10.1002/joc.3887

Bontogho, T.-N.P., Kansole, M.M., Kabore, M., Guira, M. 2023. Comparative analyses of SPI and SPEI as drought characterization tools in Massili watershed, central Burkina Faso. Int. J. Hydrol. Res. 8: 14–22. doi:10.18488/ijhr.v8i1.3485

Boonwichai, S., Shrestha, S., Babel, M.S., Weesakul, S., Datta, A. 2018. Climate change impacts on irrigation water requirement, crop water productivity, and and rice yield in the Songkhram River Basin, Thailand. J. Clean. Prod. 198: 1157–1164. doi.org/10.1016/j.jclepro.2018.07.179

Boonwichai, S., Shrestha, S., Pradhan, P., Babel, M.S., Datta, A. 2021. Adaptation strategies for rainfed rice water management under climate change in Songkhram River Basin, Thailand. J. Water Clim. Change. 12: 2181–2198. doi.org/10.2166/wcc.2021.152

Cadro, S., Uzunovic, M. 2013. How to use: package 'SPEI' for basic calculations. https://www.researchgate.net/publication/299971042_HOW_TO_USE_Package_%27SPEI%27_For_BASIC_CALCULATIONS, 4 March 2025.

Cardoso de Salis, H.H., Monteiro da Costa, A., Moreira Vianna, J.H., Schuler, M., Künne, A., Sanches Fernandes, L.F., Leal Pacheco, F.A. 2019. Hydrologic modeling for sustainable water resources management in urbanized Karst areas. Int. J. Environ. Res. Public Health. 16: 2542. doi.org/10.3390/ijerph16142542

Department of Disaster Prevention and Mitigation (DDPM). 2025. Report on disaster-affected areas, declaration of disaster-affected zones, and and declaration of emergency disaster relief areas. https://datacenter.disaster.go.th/datacenter/cms?id=8532, 13 March 2025.

Foyhirun, C., Promping, T. 2021. Future hydrological drought hazard assessment under climate and land use projections in the Upper Nan River Basin, Thailand. Eng. Appl. Sci. Res. 48: 781–790. doi.org/10.14456/easr.2021.61

Gebre, S.L. 2015. Application of the HEC-HMS model for runoff simulation of Upper Blue Nile River Basin. Hydrol. Curr. Res. 6. doi.org/10.4172/2157-7587.1000183

Ghimire, U., Shrestha, S., Neupane, S., Mohanasundaram, S., Lorphensri, O. 2021. Climate and land-use change impacts on spatiotemporal variations in groundwater recharge: A case study of the Bangkok area, Thailand. Sci. Total Environ. 792:148370. doi.org/10.1016/j.scitotenv.2021.148370

Gupta, H.V., Sorooshian, S., Yapo, P.O. 1999. Status of automatic calibration for hydrologic models: Comparison with multilevel expert calibration. J. Hydrol. Eng. 4: 135–143. doi.org/10.1061/(ASCE)1084-0699(1999)4:2(135)

Hargreaves, G.H., Allen, R.G. 2003. History and evaluation of Hargreaves evapotranspiration equation. J. Irrigat. Drain. Eng. 129: 53–63. doi:10.1061/(asce)0733-9437(2003)129:1(53)

Homdee, T., Pongput, K., Kanae, S. 2016. A comparative performance analysis of three standardized climatic drought indices in the Chi River Basin, Thailand. Agric. Nat. Resour. 50: 211–219. doi.org/10.1016/j.anres.2016.04.006

Hydro-Informatics Institute (HII). 2025. Operations in data collection and analysis for the development of a data warehouse system for 25 river basins and flood-drought simulation models - Chi River Basin. https://tiwrm.hii.or.th/web/attachments/25basins/04-chi.pdf, 13 March 2025.

IPCC. 2021. Summary for policymakers. In: Climate Change 2021: The Physical Science Basis. Contribution of Working Group I to the Sixth Assessment Report of the Intergovernmental Panel on Climate Change. [Masson-Delmotte, V., Zhai, P., Pirani, A., et al. (Eds.)]. Cambridge University Press. Cambridge, UK and New York, NY, USA. doi.org/10.1017/9781009157896.001

Janecka, K., Metslaid, S., Metslaid, M., Harvey, J.E., Wilmking, M. 2022. Short-term effects of droughts and cold winters on the growth of Scots Pine at coastal sand dunes around the South Baltic Sea. Forests 13: 477. doi.org/10.3390/f13030477

Katipoğlu, O.M., Acar, R., Şengül, S. 2020. Comparison of meteorological indices for drought monitoring and evaluating: A case study from Euphrates Basin, Turkey. J. Water Clim. Change. 11: 29–43. doi.org/10.2166/wcc.2020.299

Kuntiyawichai, K., Sri-Amporn, W., Wongsasri, S., Chindaprasirt, P. 2020. Anticipating potential climate and land use change impacts on floods: A case study of the Lower Nam Phong River Basin. Water 12: 1158. doi.org/10.3390/w12041158

Kuntiyawichai, K., Wongsasri, S. 2021. Assessment of drought severity and vulnerability in the Lam Phaniang River Basin, Thailand. Water 13: 2743. doi.org/10.3390/w13192743

Legates, D.R., McCabe, G.J. 1999. Evaluating the use of "goodness-of-fit" measures in hydrologic and hydroclimatic model validation. Water Resour. Res. 35: 233–241. doi.org/10.1029/1998WR900018

McKee, T.B., Doesken, N.J., Kleist, J. 1993. The relationship of drought frequency and duration to time scales. Proceedings of the 8th Conference on Applied Climatology., Anaheim,. CAalifornia, USA., pp. 179–184.

Meseguer-Ruiz, O., Serrano-Notivoli, R., Aránguiz-Acuña, A., Fuentealba, M., Nuñez-Hidalgo, I., Sarricolea, P., Garreaud, R. 2024. Comparing SPI and SPEI to detect different precipitation and temperature regimes in Chile throughout the last four decades. Atmos. Res. 297: 107085. doi:10.1016/j.atmosres.2023.107085

Moriasi, D.N., Arnold, J.G., Van Liew, M.W., Bingner, R.L., Harmel, R.D., Veith, T.L. 2007. Model evaluation guidelines for systematic quantification of accuracy in watershed simulations. Trans. ASABE. 50: 885–900. doi.org/10.13031/2013.23153

Nash, J.E., Sutcliffe, J.V. 1970. River flow forecasting through conceptual models: Part I – A discussion of principles. J. Hydrol. 10: 282–290. doi.org/10.1016/0022-1694(70)90255-6

Nouri, M. 2023. Drought assessment using gridded data sources in data-poor areas with different aridity conditions. Water Resour. Manag. 37: 4327–4343. doi.org/10.1007/s11269-023-03184-3

Ojha, S.S., Singh, V., Roshni, T. 2021. Comparative analysis of meteorological drought based on the SPI and SPEI indices in Benin. Civil Eng. J. 7: 2130–2149. doi.org/10.28991/cej-2021-03091785

Öz, F.Y., Özelkan, E., Tatlı, H. 2024. Comparative analysis of SPI, SPEI, and RDI indices for assessing spatio-temporal variation of drought in Türkiye. Earth Sci. Inform. 17: 4473–4505. doi.org/10.1007/s12145-024-01401-8

Pathak, A.A., Dodamani, B.M. 2019. Comparison of meteorological drought indices for different climatic regions of an Indian River Basin. Asia-Pac. J. Atmos. Sci. 56: 563–576. doi.org/10.1007/s13143-019-00162-5

Pei, Z., Fang, S., Wang, L., Yang, W. 2020. Comparative analysis of drought indicated by the SPI and SPEI at various timescales in Inner Mongolia, China. Water. 12: 1925. doi.org/10.3390/w12071925

Prakongsri, P., Santiboon, T. 2020. Effective water resources management for communities in the Chi River Basin in Thailand. Environ. Claims J. 32: 323–348. doi.org/10.1080/10406026.2020.1755637

Promping, T., Tingsanchali, T. 2020. Meteorological drought hazard assessment under future climate change projection for agricultural areas in the Songkhram River Basin, Thailand. Proceeding of the 2020 International Conference and Utility Exhibition on Energy, Environment and Climate Change (ICUE). Pattaya, Thailand., pp. 1–7.

Promping, T., Tingsanchali, T. 2025. A method for formulating a new composite drought hazard index for assessment of multiple drought hazards under projected climate and land use changes in agricultural areas: A case of Wang River Basin, Thailand. Nat Hazards. 121: 3343–3374. doi.org/10.1007/s11069-024-06886-6

R Core Team. 2024. R: A Language and Environment for Statistical Computing. R Foundation for Statistical Computing. https://www.R-project.org/, 13 March 2025.

Rashid, MdM., Beecham, S. 2019. Development of a non-stationary Standardized Precipitation Index and its application to a South Australian climate. Sci. Total Environ. 657: 882–892. doi.org/10.1016/j.scitotenv.2018.11.304

Schulze, R.E. 2000. Modelling hydrological responses to land use and climate change: A Southern African perspective. AMBIO: J. Hum. Environ. 29: 12–22. doi.org/10.1639/0044-7447(2000)029[0012]2.0.CO;2

Shah, R., Bharadiya, N., Manekar, V. 2015. Drought index computation using Standardized Precipitation Index (SPI) method for Surat District, Gujarat. Aquatic Procedia. 4: 1243–1249. doi.org/10.1016/j.aqpro.2015.02.161

Shrestha, A., Shrestha, S., Tingsanchali, T., Budhathoki, A., Ninsawat, S. 2021. Adapting hydropower production to climate change: A case study of Kulekhani Hydropower Project in Nepal. J. Cleaner Prod. 279: 123483. doi.org/10.1016/j.jclepro.2020.123483

Shrestha, S., Bajracharya, A.R., Babel, M.S. 2016. Assessment of risks due to climate change for the Upper Tamakoshi Hydropower Project in Nepal. Climate Risk Manage. 14: 27–41. doi.org/10.1016/j.crm.2016.03.003

Shrestha, S., Neupane, S., Mohanasundaram, S., Pandey, V.P. 2020. Mapping groundwater resiliency under climate change scenarios: A case study of Kathmandu valley, Nepal. Environ. Res. 183:109149. doi:10.1016/j.envres.2020.109149

Suroso, N., Nadhilah, D., Ardiansyah, A., Aldrian, E. 2021. Drought detection in Java Island based on Standardized Precipitation and Evapotranspiration Index (SPEI). J. Water Clim. Change. 12: 2734–2752. doi.org/10.2166/wcc.2021.225

Svoboda, M., Fuchs, B. 2016. Handbook of drought indicators and indices. Integrated Drought Management Programme (IDMP). Drought Mitigation Center Faculty Publications.

Tefera, A.S., Ayoade, J.O., Bello, N.J. 2019. Comparative analyses of SPI and SPEI as drought assessment tools in Tigray Region, Northern Ethiopia. SN Appl. Sci. 1: 1265. doi.org/10.1007/s42452-019-1289-2

Thom, H.C.S. 1996. Some methods of climatological analysis. Secretariat of the World Meteorological Organization. Geneva, Switzerland. pp.53

Tirivarombo, S., Osupile, D., Eliasson, P. 2018. Drought monitoring and analysis: Standardised precipitation evapotranspiration index (SPEI) and Standardized Precipitation Index (SPI). Phys. Chem. Earth, Parts A/B/C, 106: 1–10. doi:10.1016/j.pce.2018.07.001

Vicente-Serrano, S.M., Begueria, S., Lopaz-Moreno, J.I. 2010. A multiscalar drought index sensitive to global warming: The Standardized Precipitation Evapotranspiration Index. J. Climate. 23: 1696–1718. doi.org/10.1175/2009JCLI2909.1

Walz, Y., Wegmann, M., Dech, S., Vounatsou, P., Poda, J.N., N'goran, E.K., Utzinger, J., Raso, G. 2015. Modeling and validation of environmental suitability for schistosomiasis transmission using remote sensing. PLOS Negl. Trop. Dis. 9: 1–22. doi.org/10.1371/journal.pntd.0003520

Wang, W., Lu, Y. 2017. Analysis of the Mean Absolute Error (MAE) and the Root Mean Square Error (RMSE) in assessing rounding models. Proceeding of the 5th International Conference on Mechanical Engineering, Materials Science and Civil Engineering., Kuala Lumpur, Malaysia, pp. 012049.

WMO, GWP. 2016. Handbook of drought indicators and indices (Svoboda, M. and Fuchs, B.A.). Integrated Drought Management Programme (IDMP): Integrated Drought Management Tools and Guidelines Series 2. Geneva, Switzerland.

Yalçın, S., Eşit, M., Çoban, Ö. 2023. A new deep learning method for meteorological drought estimation based on Standardized Precipitation Evapotranspiration Index. Eng. Appl. Artif. Intell. 124: 106550. doi.org/10.1016/j.engappai.2023.106550

Yang, G., Guo, S., Li, L., Hong, X., Wang, L. 2016. Multi-objective operating rules for Danjiangkou reservoir under climate change. Water Resour. Manag. 30: 1183–1202. doi.org/10.1007/s11269-016-1275-0

Zhao, F., Xu, Z., Zhang, L., Zuo, D. 2009. Streamflow response to climate variability and human activities in the upper catchment of the Yellow River Basin. Sci. China Ser. E: Technol. Sci. 52: 3249–3256. doi.org/10.1007/s11431-009-0315-0